AJNR

This information is current as of May 28, 2025.

Apparent Diffusion Coefficient Determination in Normal Fetal Brain: A Prenatal MR Imaging Study

Andrea Righini, Elena Bianchini, Cecilia Parazzini, Patrizia Gementi, Luca Ramenghi, Cristina Baldoli, Umberto Nicolini, Fabio Mosca and Fabio Triulzi

Apparent Diffusion Coefficient Determination in Normal Fetal Brain: A Prenatal MR Imaging Study

Andrea Righini, Elena Bianchini, Cecilia Parazzini, Patrizia Gementi, Luca Ramenghi, Cristina Baldoli, Umberto Nicolini, Fabio Mosca, and Fabio Triulzi

BACKGROUND AND PURPOSE: Diffusion-weighted MR imaging studies of normal brain development have focused on premature babies who were free of focal lesions on conventional MR images. The condition of prematurity, however, is dissimilar to intrauterine life. We sought to establish normal values of fetal brain apparent diffusion coefficient (ADC) to highlight its abnormal changes in pathologic conditions and to obtain information about normal brain development.

METHODS: We measured the ADC, in utero, by using an echo-planar three-axes diffusion-sensitized sequence (b factor, 0 and 600 s/mm^2), in frontal and occipital white matter and basal ganglia gray matter of 15 fetuses. Their gestational ages ranged from 22 to 35 weeks, and the postnatal MR images or sonograms revealed normal brain.

RESULTS: Mean ADC value was 1.96 ± 0.1 μm^2/ms (SD) in frontal white matter, 1.95 ± 0.1 μm^2/ms in occipital white matter, and 1.56 ± 0.1 μm^2/ms in basal ganglia. A significant negative correlation between ADC and gestational age was found for basal ganglia, whereas only a trend was present for frontal white matter.

CONCLUSION: Although moderately higher, the ADC determinations we obtained are consistent with those reported in the literature in postnatal studies performed in premature babies.

The measurement of water apparent diffusion coefficient (ADC) in the human brain by means of diffusion-weighted (DW) MR imaging has provided valuable information in adults with stroke, seizures, trauma, or white matter disorders (1–4). In premature and full-term neonates, DW imaging has allowed observations to be obtained not only in certain brain diseases, such as global hypoxia-ischemia (5–8) or periventricular leukomalacia (9), but also in normal cerebral development (10–13). Prenatal MR imaging is widely used to assess fetal brain abnormalities in cases of unclear or incomplete prenatal sonographic (US) results. In particular, prenatal US has poor sensitivity in the detection of acute lesions, such as the early stages of hypoxic-ischemic damage (14), which is one of the leading causes of fetal brain

destructive processes. Prenatal DW imaging enabled detection of acute fetal brain ischemic lesions in a very recent report (15). We thought it would be worthwhile to establish the normal values of fetal brain ADC not only to highlight abnormal changes in pathologic conditions, but also to add information about normal brain development. DW imaging studies on normal brain development have focused, so far, on premature babies who were free from focal lesions noticeable on conventional MR images (11–13). Despite the high quality and high spatial resolution of such imaging data, the condition of prematurity is far from being similar to intrauterine life. For these reasons, we measured the ADC in cerebral white and gray matter of fetuses with a normal brain and whose gestational ages ranged from 22 to 35 weeks.

Methods

Subjects

Among consecutive prenatal MR imaging studies routinely performed for clinical purposes at our institution from January 2001 to March 2002, the images of 15 fetuses were included in the study. All mothers signed an informed consent form. The following inclusion criteria were adopted: 1) fetuses imaged because of clinical and US suspicion of anomalies in organs other than the fetal brain, but with normal brain at prenatal US

Demographic and clinical data

Fetus No.	Mother's Age (y)	Gestational Age (wks)	Clinical or Prenatal Problem at US	Prenatal Brain T2-Weighted SS FSE Findings	Postnatal Brain MR or US Findings
1	34	30	Intestinal occlusion	Normal	Normal (US)
2	32	32	Mega–cisterna magna	Mega–cisterna magna	Posterior fossa arachnoid cyst; normal cerebellum vermis, and cerebral hemispheres (MR)
3	35	24	TTTS, larger (receiver) twin studied	Normal	Normal (MR)
4	33	28	TTTS, larger (receiver) twin studied	Normal	Normal (MR)
5	23	29	Mega–cisterna magna	Mega–cisterna magna	Mega–cisterna magna; normal cerebellum, vermis, and cerebral hemispheres (MR)
6	27	34	Neck mass	Normal	Normal (US) (neck cystic hygroma at surgery)
7	35	24	Lumbar hemivertebrae	Normal	Not available (pregnancy terminated; skeletal malformations, no meningocele, and normal brain at autopsy; normal chromosomic map).
8	28	25	Facial anomalies	Normal	Normal (US) (facial anomalies not confirmed)
9	37	23	Two previous pregnancies with corpus callosum agenesis	Normal	Normal (US)
10	31	29	Intestinal occlusion	Normal	Normal (US)
11	37	22	Pulmonary adenoid cystic malformation	Normal	Normal (US)
12	29	32	Amnionic bands and oligohydramnios	Normal	Normal (US)
13	34	25	Diaphragmatic herniation	Normal	Normal (MR)
14	32	35	Focal hepatic lesion	Normal	Normal (US)
15	37	22	One previous pregnancy with corpus callosum agenesis	Normal	Normal (US)

Note.—TTTS indicates twin-to-twin transfusion syndrome; SS FSE, single-shot fast spin echo.

and at T2-weighted single-shot fast spin-echo (SE) MR imaging (nine cases); 2) fetuses imaged with prenatal MR imaging because of the risk of possible brain damage, but with normal prenatal brain sonograms, as in twin-to-twin transfusion syndrome, and resulting in negative prenatal T2-weighted single-shot fast SE MR images (two cases); 3) fetuses imaged with prenatal MR imaging because brain anomalies had been noted in previous pregnancies, such as corpus callosum agenesis, but with normal prenatal sonograms and resulting in negative prenatal T2-weighted single-shot fast SE MR images (two cases); and 4) fetuses imaged because of suspected mild intracranial anomalies at prenatal US such as widening of cisterna magna and with otherwise normal prenatal sonograms and prenatal T2-weighted single-shot fast SE MR images (two cases). All pregnancies were free from history of maternal diabetes or hypertension. All neonates had a normal neurologic examination. In all but one case (fetus 7 in Table), postnatal sonograms or MR images were available and evaluated separately by three pediatric neuroradiologists (A.R., E.B., and C.P.), who confirmed normal brain findings, with the exception of the two cases in criterion 4, who showed widening of cisterna magna and posterior fossa arachnoid cyst at postnatal MR imaging, respectively. We decided to include these two cases because postnatal findings related to cerebellar and cerebral morphology and parenchymal signal intensity were unremarkable, as was the neurologic examination. Although it is well known that the time course of normal brain development can present some delay in twins, we also included the two cases of twin-to-twin transfusion syndrome because their ADC values were similar to the ones of the singletons of the same gestational age.

Mean maternal age was 32.3 ± 4.1 years (SD), and mean gestational age of the fetuses was 27.6 ± 4.4 weeks (range, 22–35 weeks) (Table).

MR Imaging and Data Analysis

All MR imaging was performed with a 1.5-T unit (Horizon LX, Echospeed; GE Medical Systems, Milwaukee, WI). No sedation of the mother or fetus was required. For conventional prenatal MR imaging, a body dedicated phased-array coil was used, and no breath holding was required of the mother. Multiplanar T2-weighted single-shot fast SE 3–5-mm-thick sections were acquired with the following parameters: TR, indefinite; TE, 90 ms; field of view, 320–380 mm; matrix, 256 × 192. For DW imaging, we switched to the whole-body coil (without repositioning the mother), because on our system phased-array coils did not allow performance of echo-planar DW imaging. By using sagittal T2-weighted single-shot fast SE sections as a scout view, axial single-shot echo-planar DW imaging sections were prescribed on fetal brain. The DW sequence, which had an acquisition time of 20 seconds, was performed with breath holding by the mother. Because of frequent image motion degradation, usually two or three DW sequence acquisitions had to be performed before obtaining satisfactory images. DW imaging section thickness varied from 5 to 6 mm according to fetal head size. Other parameters were 5000/81 (TR/TE), field of view of 320 mm, and matrix of 128 × 128, leading to an in-plane resolution of 2.5 × 2.5 mm. The sensitizing diffusion gradients were applied on the three (x, y, z) orthogonal axes with two b factors (0 and 600 s/mm^2) per axis.

Rotational relatively insensitive mean diffusivity maps (trace ADC maps) were then calculated by using a standard software (Func tool) running on the imager's main console. For each case, a pediatric neuroradiologist (A.R.), after selecting the better motion artifact–free DW section at the level of basal ganglia, traced circular regions of interest (ROIs) on the corresponding echo-planar (b = 0 s/mm^2, T2-weighted) image in the basal ganglia, frontal white matter, occipital white matter, and CSF of the lateral ventricles (Fig 1). ROI sizes varied from
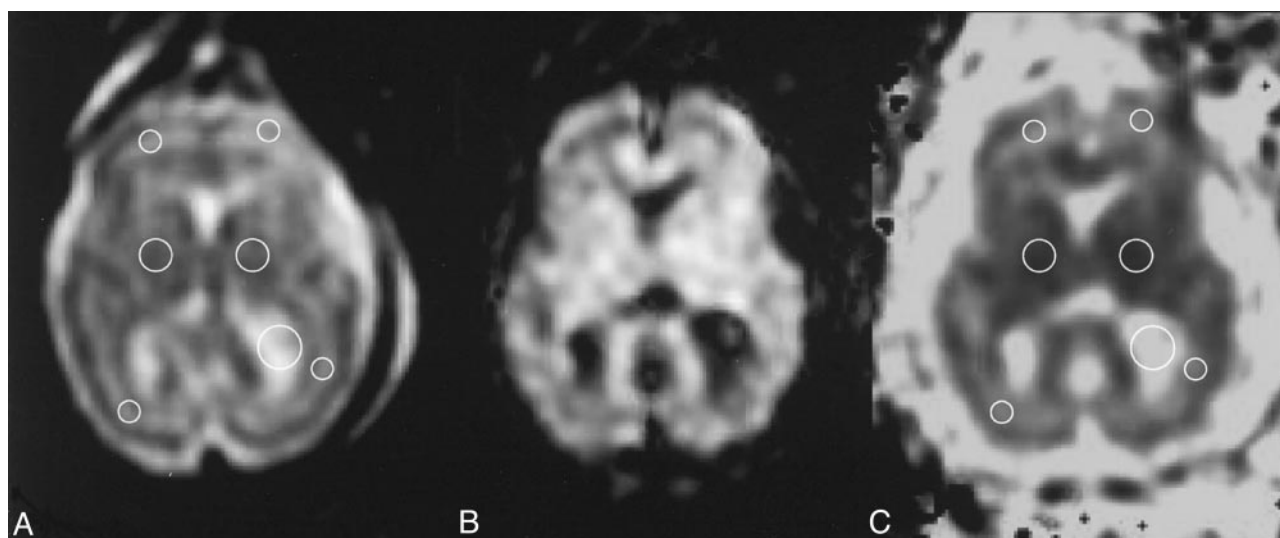
FIG 1.　Representative case (fetus 10 in Table). *A*, T2-weighted echo-planar image (b = 0 s/mm^2), *B*, corresponding DW image, and *C*, resultant trace ADC map illustrate typical ROIs (circles in *A* and *C*) traced on an axial section at the basal ganglia level.

30 to 50 mm^2 and 40 to 80 mm^2 for the white matter and basal ganglia regions, respectively, according to the gestational age and size of the fetal brain. From the image obtained with b = 0 s/mm^2, ROIs were then automatically transferred onto the trace ADC map. The ROI values for frontal white matter were available in 13 of the 15 cases; for occipital white matter, in 14 cases; and for basal ganglia, in 13 cases. Since no statistically significant difference was found between the ROI values of the right and left hemispheres, the average between ROI values of both hemispheres was considered for final statistics. To assess statistically significant differences between the mean ADC value in the ROIs traced, a paired *t* test was used, and *p* < .05 was considered a statistically significant difference.

Results

The mean ADC value was 1.96 ± 0.1 μm^2/ms (SD) in frontal white matter, 1.95 ± 0.1 μm^2/ms in occipital white matter, and 1.56 ± 0.1 μm^2/ms in basal ganglia; the difference between basal ganglia and both frontal and occipital white matter was statistically significant (*P* < .0001, paired *t* test). The mean ADC value in CSF was 3.1 ± 0.1 μm^2/ms (Fig 2). A significant

negative correlation between ADC values and gestational age could not be found for frontal and occipital white matter, although there was a trend in this sense for frontal white matter. A significant negative correlation with gestational age was found for the basal ganglia ROIs (Fig 3).

Discussion

DW imaging and ADC determinations are feasible in fetal brain by using prenatal MR imaging. This type of study is intrinsically more difficult than postnatal studies, since image degradation due to mother-fetal motion artifact and to aorta pulsatility effects may require more than one acquisition to be repeated to obtain satisfactory images. The signal-to-noise ratio and the spatial resolution are not as good as those obtained with postnatal imaging in infants and in adult imaging. However, the ADC determinations we obtained are consistent with those reported in postnatal studies performed in premature babies (11–13). Moreover, our ADC values for CSF are similar to what has been reported in neonates and adult ventricles (12, 16), supporting the consistency of our measurements. The mean ADC value for white matter ROIs was higher than that of the basal ganglia gray matter, as already demonstrated by previous studies in premature neonates (12, 13). The explanation for this is not totally clear, but it could be because gray matter has more cells and membranes per volume unit that unmyelinated white matter, and the interstitial water is more abundant in the latter.

The average ADC values for both white and gray matter in our study were moderately higher than those reported in premature neonate DW imaging studies (range of means for white matter, approximately 1.8–1.9 μm^2/ms; range of means for basal ganglia gray matter, approximately 1.2–1.3 μm^2/ms) (11–13). The reason for this discrepancy is not clear. The mean gestational age of our fetuses was moder-
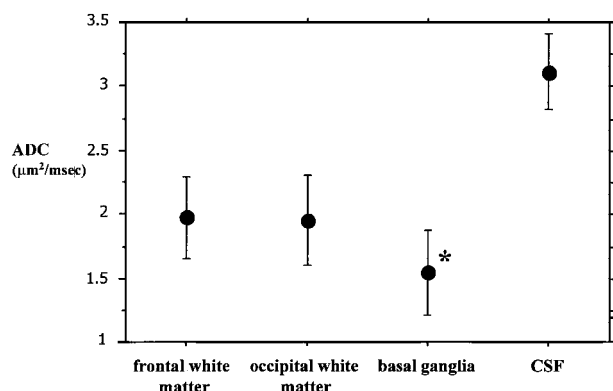

FIG 2.　Graph shows the mean ADC values (bars indicate 2 SDs) for frontal and occipital white matter, basal ganglia, and CSF ROIs. The mean ADC of basal ganglia is significantly lower than that of white matter ROIs. * indicates *P* < .0001 (paired *t* test).
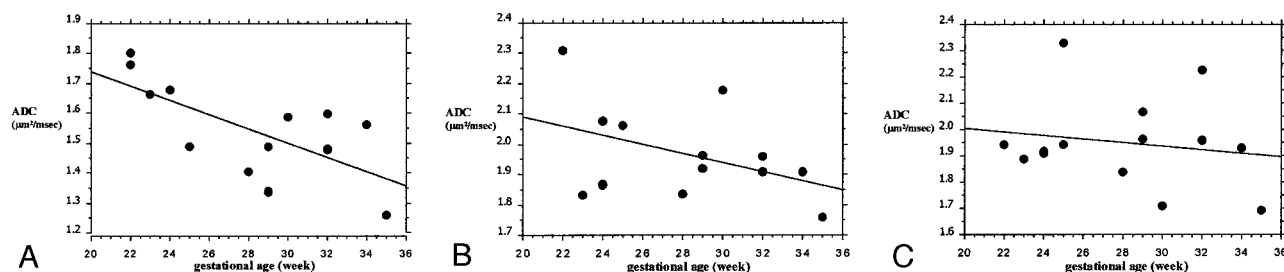
FIG 3. Graphs show the correlation between ADC values for the ROIs traced and gestational age. A significant negative correlation was present only for the basal ganglia ROI.
A, Basal ganglia: $Y = 2.222 - 0.024X$; $R^2 = 0.471$; $P = .0096$.
B, Frontal white matter: $Y = 2.394 - 0.015X$; $R^2 = 0.182$; $P = .1457$.
C, Occipital white matter: $Y = 2.14 - 0.007X$; $R^2 = 0.028$; $P = .5654$.

ately lower than the postconceptional age of the premature neonates reported, and this could have resulted in moderately higher ADC values in our study. The possibility of partial volume effect also has to be taken into account. In particular, since our spatial resolution was quite coarse, frontal and occipital white matter ROIs may have been contaminated by the adjacent cortical CSF, resulting in higher ADC values. However, if this is true for the white matter ROIs, it is very unlikely for basal ganglia ROIs, which were clear from CSF spaces. An additional explanation for the mentioned discrepancy is the important difference in biologic enviroment between a fetus and a premature neonate of similar age. The physiologic phenomenon of dehydration during the first days following birth, regardless of gestational age, should also be considered, as none of the studies on premature babies could be performed very close to birth. In addition, the dispersion of water after birth can also be influenced by a marked instability in the control of total body water, which can be exacerbated by the changing clinical conditions (17).

Previous studies (11, 13) reported a significant negative correlation between ADC values and postconceptional age. Their regression analysis included measurements in both premature and full-term neonates. Looking exclusively at their data on premature babies (younger than 36 weeks' postconceptional age), the significance of the negative correlation between age and ADC may be questioned, although a consistent trend is undoubtedly present. We did find a significantly negative correlation between ADC value and gestational age only for gray matter (basal ganglia), although a trend for frontal white matter was noticeable. The explanations for this ADC progressive decrease that we can provide are similar to what has been reported by authors of previous human (11, 13) and animal (18) studies: a progressive reduction in total water content within the brain and a rising in lipid concentrations, as shown by pathology data (19); an increase in the concentration of macromolecules within the intracellular compartment; and a greater membrane surface-to-cell volume ratio (18). Moreover, recent data about T2 measurements in the brains of premature babies (20) show also that the T2 value significantly decreases with postconceptional age, so at least in part both T2 and ADC changes are

probably related to the aforementioned tissular modifications. Although a trend of negative correlation between gestational age and ADC was evident in frontal white matter but not in the occipital white matter, we cannot draw consistent conclusions from that, in particular regarding the apparent discrepancy between these data and the fact that white matter maturation and myelination are well known to occur with an occipital-to-frontal gradient direction. Partial volume effects with the adjacent CSF could have affected the occipital white matter ROIs more than the frontal white matter ROIs, since the frontal white matter was generally thicker than the occipital white matter. Moreover, the small number of subjects studied, which is one of the limitations of our study, is probably not sufficient to establish a robust correlation between gestational age and white matter ADC. It is likely that further studies, including more subjects and using higher spatial resolution imaging, would confirm a negative correlation to be present between gestational age and ADC in both frontal and occipital white matter.

The ROIs we traced in the white matter, in particular in the frontal area, probably also included, in many of our cases, those periventricular areas containing the so-called bands of migrating glia, originally described in anatomic tables by Feess-Higgins and Larroche (21). In this sense, the fetal white matter is certainly not as uniform in structure as the adult and fully myelinated white matter. One MR imaging study (22) in premature babies has clearly defined the location and extension of such bands of migrating glia and their temporal evolution; the bands seem to be a very important marker of normal brain development, in particular of the white matter, as these glial precursors will transform into more mature astrocytes (most) and only a small part will reach the cortex to reinforce the lowest layer of the cortical glia (23). In our study, even though the frontal white matter ROIs included part of these bands, the ADC values of frontal and occipital white matter did not differ significantly, probably because the limited resolution of our images yielded an average between the ADC of such bands and the ADC of the rest of frontal white matter. If these areas containing the bands of migrating glia were investigated with a higher spatial resolution and a more sophisticated technique, such as

diffusion tensor imaging, their relative anisotropy index and ADC would probably be different from those of other white matter areas.

Because of the relatively coarse resolution of the echo-planar images we obtained, it is possibile also that the basal ganglia ROI meaurements might have been affected by partial volume problems, in particular for the inclusion of some adjacent white matter areas like the posterior limb of the internal capsule. However, previous work in the premature age range (11) has shown that ADC measurements in the posterior limb of the internal capsule tend not to vary significantly with postconceptional age, probably because of the already advanced myelination process of this structure, so this partial volume effect should have affected the ADC values of basal ganglia ROIs in our cases in a constant manner.

To obtain better signal-to-noise ratio on DW images in the present study, we used a b factor maximum value of only 600 s/mm^2, similar to previous studies in premature neonates (11). Recent work on neonate and adult brains (24) has confirmed the presence of a slow and a fast component of the ADC decay curve. The ADC decay curve related to the neonate brain has a significantly higher fraction of the fast diffusion component with respect to that of the adult brain. The use of relatively lower b factor values, such as in our study, may therefore be preferred in investigating normal fetal brain, since the left portion of the ADC decay curve (fast component) prevails. However, in case of pathologic ADC reduction, as in acute ischemia, when the slow component prevails, the use of lower b values might underestimate the degree of ADC reduction.

One of the main limitations of this study is that it does not deal with the important issue of white matter anisotropy and its variations along with brain maturation, as shown by previous investigations in neonates (11, 13, 25). Our ADC determination was not completely rotationally insensitive, since three-axis DW imaging acquisition cannot accurately explore the preferential diffusivity within each voxel. In the aforementioned studies in neonates, technically adequate acquisitions were based on at least six-axis diffusion gradients, to allow a complete spatial characterization of the diffusion tensor for each voxel. In these studies, brain maturation was associated with an increase in white matter anisotropy index, which was noticeable even in areas known from histologic examination to be not yet myelinated: the so called premyelination maturation process or premyelinating state. This premyelinating state is characterized by increase in axon diameter, axonal membrane changes, increased concentration of microtubule-associated proteins, and early wrapping of axons by oligodendroglial processes (11, 26).

Technical and methodological improvements in fetal DW imaging, such as the use of surface coils, will allow better spatial resolution and signal-to-noise ratio images to be obtained. Sequences exploring the preferential water diffusivity on more than six axes and allowing diffusion tensor determination will probably provide valuable and more detailed information about white matter maturation, during both the myelinating and premyelinating processes; however, the need for breath-hold images in pregnant women remains an obstacle, as does the difficulty of performing so rapid (breath-hold compatible) diffusion tensor imaging acquisitions.

Even if MR imaging has been routinely and widely used in fetal imaging in the last 10 years (27) and the subjects we studied had already been scheduled for clinical imaging, the safety issue of prenatal MR imaging should be mentioned, in particular in relation to the use of echo-planar imaging sequences. Few studies have so far focused on the safety issue regarding the use of MR imaging in human fetal imaging. One in particular by Baker and colleagues (28) investigated the potential long-term adverse effects of echo-planar imaging in children who had been imaged in utero. Their data, however, did not demonstrate any future anomaly, including hearing damage, related to intrauterine exposure to echo-planar imaging.

The present study provides information about brain ADC values in normal fetuses of the gestational age range that usually applies also to fetuses imaged for suspected cerebral malformations or destructive lesions. It would be of interest to explore possible abnormal ADC variations in fetuses with major cerebral malformations or with severe intrauterine growth retardation.

Addendum: Phantom Study

A phantom test was conducted to assess if the ADC measurements we obtained in fetuses by using the whole-body coil were comparable to those obtained in premature neonates during routine clinical studies, which are usually performed with a standard quadrature head coil. A corn oil phantom was imaged by using the whole-body coil and the standard quadrature head coil; all the DW imaging acquisition parameters were the same as for the fetal MR imaging protocol. At 22.5°C and after 10 measurements, the mean ADC value obtained with the whole-body coil (0.46 $\pm$ 0.03 μm^2/ms) was similar to that obtained with the quadrature head coil (0.43 $\pm$ 0.02 μm^2/ms).

Acknowledgments

References

1. Warach S, Chien D, Li W, et al. **Fast magnetic resonance diffusion-weighted imaging of acute human stroke**. *Neurology* 1992;42:1717–1723
2. Kim JA, Chung JI, Yoon PH, et al. **Transient MR signal changes in patients with generalized tonicoclonic seizure or status epilepticus: periictal diffusion-weighted imaging**. *AJNR Am J Neuroradiol* 2001;22:1149–1160
3. Liu AY, Maldjian JA, Bagley LJ, Sinson GP, Grossman RI. **Traumatic brain injury: diffusion-weighted MR imaging findings**. *AJNR Am J Neuroradiol* 1999;20:1636–1641
4. Roychowdhury S, Maldjian JA, Grossman RI. **Multiple sclerosis: comparison of trace apparent diffusion coefficients with MR enhancement pattern of lesions**. *AJNR Am J Neuroradiol* 2000;21:869–874

5. Cowan FM, Pennock JM, Hanrahan JD, et al. **Early detection of cerebral infarction and hypoxic-ischemic encephalopathy in neonates using diffusion-weighted magnetic resonance imaging.** *Neuropediatrics* 1994;25:172–175

6. Johnson AJ, Lee BC, Lin WL. **Echoplanar diffusion-weighted imaging in neonates and infants with suspected hypoxic-ischemic injury: correlation with patient outcome.** *AJR Am J Roentgenol* 1999;172:219–226

7. Robertson RL, Ben-Sira L, Barnes PD, et al. **MR line scan diffusion-weighted imaging of term neonates with perinatal brain ischemia.** *AJNR Am J Neuroradiol* 1999;20:1658–1670

8. Soul JS, Robertson RL, Tzika AA, du Plessis AJ, Volpe JJ. **Time course of changes in diffusion-weighted magnetic resonance imaging in a case of neonatal encephalopathy with defined onset and duration of hypoxic-ischemic insult.** *Pediatrics* 2001;108:1211–1214

9. Inder T, Huppi PS, Zientara GP, et al. **Early detection of periventricular leukomalacia by diffusion-weighted magnetic resonance imaging techniques.** *J Pediatr* 1999;134:631–634

10. Toft PB, Leth H, Peitersen B, et al. **The apparent diffusion coefficient of water in gray and white matter of the infant brain.** *J Comput Assist Tomogr* 1996;20:1006–1011

11. Huppi PS, Maier SE, Peled S, et al. **Microstructural development of human newborn cerebral white matter assessed in vivo by diffusion tensor magnetic resonance imaging.** *Pediatr Res* 1998;44:584–590

12. Tanner SF, Ramenghi LA, Ridgway JP, et al. **Quantitative comparison of intrabrain diffusion in adults and preterm and term neonates and infants.** *AJR Am J Roetgenol* 2000;174:1643–1649

13. Neil J, Shiran SI, McKinstry RC, et al. **Normal brain in human newborns: apparent diffusion coefficient and diffusion anisotropy measured by using diffusion tensor MR imaging.** *Radiology* 1998;209:57–66

14. Langer B, Boudier E, Gasser B, et al. **Antenatal diagnosis of brain damage in the survivor after second trimester death of a monochorionic monoamniotic co-twin.** *Fetal Diagn Ther* 1997;12:286–291

15. Baldoli C, Righini A, Parazzini C. et al. **Demonstration of acute ischemic lesions in the fetal brain by diffusion MRI.** *Ann Neurol* 2002;52:243–246

16. Pierpaoli C, Jezzard P, Basser PJ, Barnett A, Di Chiro G. **Diffusion tensor MR imaging of the human brain.** *Radiology* 1996;201:637–648

17. MacLaurin JC. **Changes in body water distribution during the first two weeks of life.** *Arch Dis Child* 1966;41:286–291

18. Baratti C, Barnett AS, Pierpaoli C. **Comparative MR imaging study of brain maturation in kittens with T1, T2, and the trace of the diffusion tensor.** *Radiology* 1999;210:133–142

19. Dobbing J, Sands J. **Quantitative growth and development of human brain.** *Arch Dis Child* 1973;48:757–767

20. Counsell SJ. **T2 relaxation values in the developing preterm brain (abstr).** In: *Proceedings of the Ninth Meeting of the International Society for Magnetic Resonance in Medicine 2001.* Berkeley: International Society for Magnetic Resonance in Medicine, 2001; 410

21. Feess-Higgins A, Larroche JC. *Development of the human fetal brain. An anatomical atlas.* Paris: Masson; 1987

22. Childs AM, Ramenghi LA, Evans DJ, et al. **MR features of developing periventricular white matter in preterm infants: evidence of glial cell migration.** *AJNR Am J Neuroradiol.* 1998;19:971–976

23. Marin-Padilla M. **Developmental neuropathology and impact of perinatal brain damage, II: white matter lesions of the neocortex.** *J Neuropathol Exp Neurol* 1997;56:219–235

24. Mulkern RV, Vajapeyam S, Robertson RL, et al. **Biexponential apparent diffusion coefficient parametrization in adult vs newborn brain.** *Magn Reson Imaging* 2001;19:659–668

25. Mukherjee P, Miller JH. Shimony JS, et al. **Normal brain maturation during childhood: developmental trends characterized with diffusion-tensor MR imaging.** *Radiology* 2001;221:349–358

26. Wimberger DM, Roberts TP, Barkovich AJ, et al. **Identification of "premyelination" by diffusion-weighted MRI.** *J Comput Assist Tomogr* 1995;19:28–33

27. Girard N, Raybaud C, Gambarelli D, et al. **Fetal brain MR imaging.** *Magn Reson Imaging Clin N Am* 2001;9:19–56

28. Baker PN, Johnson IR, Harvey PR, Gowland PA, Mansfield PA. **Three-year follow-up of children imaged in utero with echo-planar magnetic resonance.** *Am J Obstet Gynecol* 1994;170:32–33